TiO_2/Fe_2O_3/CNTs magnetic photocatalyst: a fast and convenient synthesis and visible-light-driven photocatalytic degradation of tetracycline

Changyu Lu[1], Weisheng Guan[1], Gehong Zhang[1], Linjing Ye[1], Ya Zhou[1], Xian Zhang[2]

[1]*School of Environmental Science and Engineering, Chang'an University, Xi'an 710054, People's Republic of China*
[2]*State Key Laboratory of Environmental Chemistry and Ecotoxicology, Research Center for Eco-Environmental Sciences, Chinese Academy of Sciences, Beijing 100085, People's Republic of China*
E-mail: guanweisheng@263.net

Published in Micro & Nano Letters; Received on 10th July 2013; Revised on 15th August 2013; Accepted on 5th September 2013

The effective visible-light-driven photocatalysis of tetracycline still remains a big challenge for scientists. In this reported work, TiO_2/Fe_2O_3/CNTs (carbon nanotubes) have been successfully synthesised by a fast and convenient method for the first time. A wide range of techniques, such as X-ray diffraction, scanning electron microscopy, transmission electron microscopy, magnetic measurements and UV–vis absorption spectroscopy were applied to characterise the obtained TiO_2/Fe_2O_3/CNTs. Moreover, the photocatalytic properties of the TiO_2/Fe_2O_3/CNTs in the degradation of tetracycline have been studied. In addition, it was found that TiO_2/Fe_2O_3/CNTs have a better reusable photocatalyst than other traditional photocatalysts by the magnetic separation recycling method.

1. Introduction: Tetracycline (TC), a well known broad-spectrum antibacterial agent widely used in human medicine and in the veterinary field, is extensively found in the aquatic environment, which poses serious threats to the ecosystem and human health by inducing proliferation of bacterial drug resistance [1]. The removal of TC from the environment has become an important issue. Unfortunately, the conventional degradation processes are often constrained by low efficiency and high cost. Recently, micro/nanometre-scale semiconductor materials have been established to be one of the most promising kinds of materials for environmental remediation [2] and to provide a good tool for the transformation and degradation of TC [3–5].

Carbon nanotubes (CNTs) have a typical hollow layered structure and are uni-dimensional quantum materials. Owing to their unique characteristics such as small size, relatively large specific area, and hollow and layered structure, CNTs have excellent electrical, mechanical and thermal properties [6–8], which can be used as molecular wires, nanometre semiconductor materials, catalyst carriers, molecules absorbent and the near field emission material and so on. The magnetic core/shell materials separation method was a new type of separation technology in the 1970s. The foundation is that magnetic nanoparticles were coated on an inorganic carrier, then magnetic materials could be separated rapidly with an external magnetic field. The convex surface of the CNTs proved to be very helpful to transfer mass or ions and support guest compounds as a substrate [9]. Therefore many useful materials have been coated or attached onto CNTs by covalent linkage, physical adsorption, chemical vapour deposition and other techniques [10–16]. Recently, magnetic nanoparticles (MNPs) of MO (where M is Mn [17], Co [18], Ni [19] or Fe [20]) and CNTs have become a promising research field, especially the combination of iron oxide nanoparticles with CNTs. It has been reported that Korneva *et al.* [21] have filled self-prepared CNTs with Fe_3O_4 nanoparticles, and the thermolysis of ferrocene could also be used to synthesise iron oxide-filled CNTs [22]. Among the various photocatalysts, TiO_2 has been known as one of the commonest and most efficient photocatalysts with its unique characteristics in band position, and its surface structure. However, TiO_2 can utilise only the photons in the wavelength shorter than 380 nm, which occupies no more than 4% of the solar spectrum [23]. By coating a layer of compact and uniform TiO_2 particles on magnetic CNTs, the photocatalysis of the composites is better than that of TiO_2 for the structure, properties of inorganic support and red-shift of the composites' absorption cutoff wavelength.

Here, we report for the first time the photocatalytic degradation of TC on TiO_2/Fe_2O_3/CNTs under visible-light. The TiO_2/Fe_2O_3/CNTs photocatalyst is prepared by a fast and convenient method which has been proposed. In addition, TiO_2/Fe_2O_3/CNTs were analysed and characterised by X-ray diffraction (XRD), scanning electron microscopy (SEM), transmission electron microscopy (TEM) and magnetic measurements. Moreover, we have also studied the properties of photoabsorption and photocatalytic degradation of the as-prepared TiO_2/Fe_2O_3/CNTs. Therefore our study is necessary and significant regarding TiO_2/Fe_2O_3/CNTs from the standpoint of practical applications.

2. Experimental

2.1. Material and methods: All the reagents were of analytical grade and were used without further purification except the CNTs and the water used was deionised. A typical synthesis process for the TiO_2/Fe_2O_3/CNTs composite photocatalyst is as follows: first, the multi-walled CNTs were dispersed in a mixed solution of concentrated sulphuric acid and concentrated nitric acid (3:1 volume ratio). The samples were sonicated in a typical ultrasound bath for 3 h. The acidic mixture containing CNTs was diluted to 25% of the original concentration. Then, the oxidised CNTs were filtered by a glass sand core filter (mixed cellulose ester, 0.45 μm pore size) with the support of a vacuum pump. The CNTs were vigorously washed several times by deionised water during filtration to reach neutral pH. Then, the CNTs were dried overnight in a vacuum oven at 50°C.

0.3 g of rarefied CNTs and 2.424 g $Fe(NO_3)_3{\cdot}9H_2O$ were stirred for 2 h in a sealed vessel in the ethanol solution (20 ml). After stirring, the solvent was evaporated to dryness at 60°C for several hours in nitrogen atmosphere. The dried sample kept reacting while it was exposed to propionic acid vapours (80°C for 15 h), and had a thermal treatment in nitrogen atmosphere for 2 h at 270°C. After being washed several times by ethanol, finally the composites were dried at 60°C under vacuum condition.

4 ml of butyl titanate and 36 ml of ethanol were stirred for 10 min in three-flasks then mixed using an electric stirrer for 10 min. We placed 200 mg Fe_2O_3/CNTs into the flask, sonicated in a typical ultrasound bath for several minutes and stirred for 10 min. Afterwards, 36 ml of ethanol was placed into a beaker, and

stirred whilst adding 3 ml of deionised water and 0.2 ml of HCl. Then, the sample in the beaker was slowly added into the flask. We kept stirring until the sample in the flask became gel at 40°C and then remained cool for 2 h. After being dried at 70°C in an air dry oven, the milled composites were incinerated in a Muffle furnace at 500°C for 4 h. After being cooled to room temperature, the composites were collected by centrifugation, then washed several times with distilled water and alcohol by an external magnetic field, respectively. The samples were dried in the vacuum oven at 70°C.

2.2. Characterisation and measurements: The composite of the TiO_2/Fe_2O_3/CNTs was observed by a scanning electron microscope (SEM, S-4800) and a transmission electron microscope (TEM, D8 ADVANCE of Germany Brooke AXS Company, wavelength for 0.15406 nm). The identification of the crystalline phase was performed using a Rigaku D/max-γB X-ray diffractometer (XRD). Magnetic measurements were conducted using a vibrating sample magnetometer (7300, Lakeshore). UV–vis diffused reflectance spectra of the samples were obtained from a UV–vis spectrophotometer (UV2550, Shimadzu, Japan).

2.3. Photocatalytic degradation of antibiotic: The photocatalytic properties of the powders were obtained at 298 K using our house-made instruments. The photochemical reactor contains 0.1 g TiO_2/Fe_2O_3/CNTs and 100 ml of 20 mg/l TC aqueous solution. To determine the initial absorbency of the samples, the reactor was kept in darkness for 30 min to reach absorption equilibrium. Then, the solution was irradiated by visible light and was aerated. The photochemical reactor was irradiated with a 300 W Xenon lamp which was located at a distance of 8 cm one side of the containing solution. The sampling analysis was conducted at 15 min intervals. TC absorption concentration was determined using the TU-1800 UV–vis spectrophotometer (Shanghai AoXi Technology Instrument Co. Ltd) by recording the variations of the absorption band maximum at $\lambda = 357$ nm (TC). The degradation rate (DR) was calculated by the formula

$$\mathrm{DR} = \left[\left(1 - A_i/A_0\right)\right] \times 100\%$$

where A_0 is the initial absorbency of the TC antibiotic waste water solution which reached absorbency balance and A_i is the absorbency of the reaction solution.

2.4. Recovery and reuse of photocatalyst: A recovery study was conducted by using a methanol/acetic acid (95:5, v/v) solution. After the photocatalyst and solvent contacted fully, the TiO_2/Fe_2O_3/CNTs were separated rapidly from the solution by a Nd–Fe–B permanent magnet. Subsequently, the supernatant solutions were removed and the TiO_2/Fe_2O_3/CNTs composites were washed by a methanol solution containing 5.0% acetic under ultrasound. To investigate the recovery of the photocatalyst, the TiO_2/Fe_2O_3/CNTs after photocatalytic degradation were reused in the experiments and the process was duplicated ten times.

3. Results and discussion: The crystallographic phase purity and elementary composition of the as-synthesised TiO_2/Fe_2O_3/CNTs were characterised by XRD. All the peaks displayed in the XRD pattern can be readily indexed to TiO_2/Fe_2O_3/CNTs which are in good agreement with the literature values (JCPDS No. 25-1402, 33-0664, 21-1272). As shown in Fig. 1, the diffraction peak at $2\theta = 26°$ can be confidently indexed as the (002) reflection of the CNTs, the other peaks in the range of $20° < 2\theta < 70°$ correspond to the (104), (116), (119), (206) and (4012) reflections of Fe_2O_3, another peak in the range of $20° < 2\theta < 70°$ corresponds to the (004), (101), (105), (116), (200), (211) and (204) reflections of

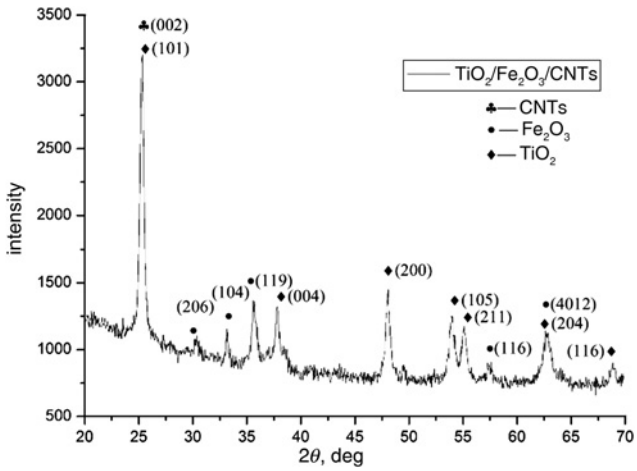

Figure 1 *XRD pattern of the typically as-synthesised TiO_2/Fe_2O_3/CNTs sample*

TiO_2. The results suggested that TiO_2 and Fe_2O_3 were introduced into the CNTs without changing their crystal structures.

Fig. 2 shows the SEM patterns of the CNTs (Fig. 2*a*), Fe_2O_3/CNTs (Fig. 2*b*), TiO_2/Fe_2O_3/CNTs (Figs. 2*c* and *d*). As depicted in Fig. 2*a*, the purified CNTs have the tendency of being bended to aggregate, even so the smooth tube wall and porous structure of the CNTs provide the probability of being support for functional application. After the Fe_2O_3 magnetic treatment, the tube wall was loaded with many nanoparticles as shown in Fig. 2*b*. From the patterns in Figs. 2*c* and *d*, Fe_2O_3/CNTs were coated with a layer of compact and uniform TiO_2 particles. The TiO_2 coating not only restrained bend and aggregation of Fe_2O_3/CNTs, but also provided photocatalysis onto the porous inorganic support.

Fig. 3 shows the TEM patterns of the CNTs (Fig. 3*a*), Fe_2O_3/CNTs (Fig. 3*b*), TiO_2/Fe_2O_3/CNTs (Figs. 3*c* and *d*). As can be seen from Fig. 3*a*, the surface of the CNTs is smooth and the diameters are ranging from 20 to 40 nm. In Fig. 3*b*, nanoparticles (Fe_2O_3 particles) with size of 10 nm on average adhered stably on the tube surface, which could be attributed to the interaction between carboxyl groups from propionic acid and ferrite nanoparticles. From Figs. 3*c* and *d*, magnetic CNTs were coated with a layer of compact and uniform particles. The TiO_2/Fe_2O_3/CNTs composite photocatalyst also has a tubular original as CNTs, and its length is greater than its diameter.

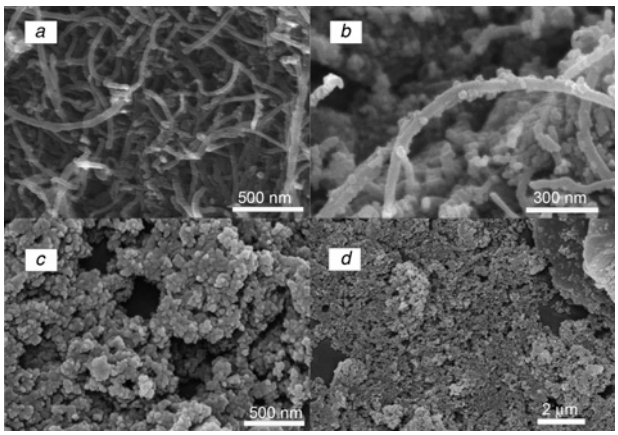

Figure 2 *SEM images*
a CNTs
b Fe_2O_3/CNTs
c and *d* TiO_2/Fe_2O_3/CNTs

doi: 10.1049/mnl.2013.0428

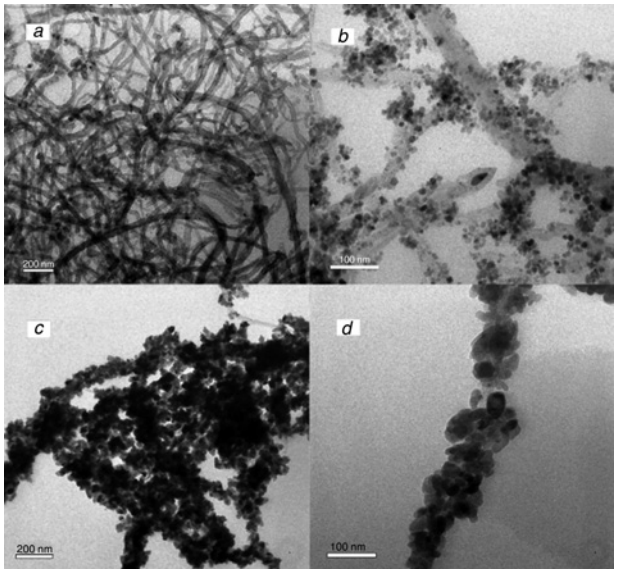

Figure 3 *TEM images*
a CNTs
b Fe_2O_3/CNTs
c and *d* TiO_2/Fe_2O_3/CNTs

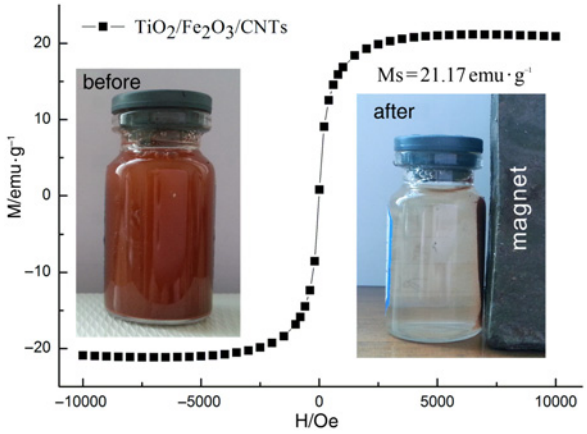

Figure 4 *Magnetisation curve of the TiO_2/Fe_2O_3/CNTs in the presence of an externally placed magnet*

Fig. 4 illustrates the magnetic hysteresis loop of the TiO_2/Fe_2O_3/CNTs. The general shape and trend of the curve indicated that the TiO_2/Fe_2O_3/CNTs were super paramagnetic. It was obvious that the saturation magnetisation (Ms) values obtained at room temperature were 21.17 emu/g for the TiO_2/Fe_2O_3/CNTs, which implied a strongly magnetic response to the external magnetic field. Furthermore, the results from Fig. 4 strongly suggested that the remaining magnetic force in the TiO_2/Fe_2O_3/CNTs could be effectively attracted by an external magnetic field, which meant that the TiO_2/Fe_2O_3/CNTs were feasible magnetic separation carriers.

As is well acknowledged, the light absorption extent plays a key role in determining the photocatalytic activity of a photocatalyst. The process of photocatalysis for a semiconductor is the direct absorption of photons by the bandgap to excite electrons from the valence band to the conduction band in particles, and the separated electrons and holes subsequently move to the particle surface and react [3]. To further understand the TiO_2/Fe_2O_3/CNTs, we have studied the UV–vis diffused reflection spectra. As shown in Fig. 5*a*, the absorption cutoff wavelength for TiO_2 is determined to be about 400 nm, which means TiO_2 only absorbs ultraviolet

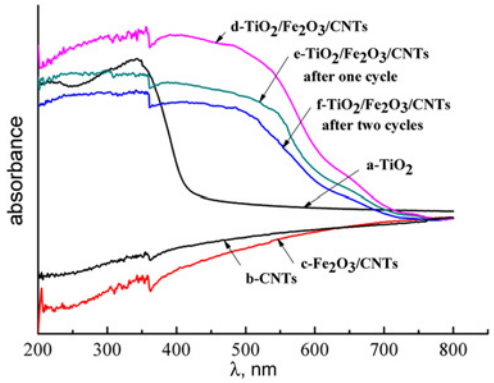

Figure 5 *UV–vis diffuse reflection absorption spectra*
a TiO_2
b CNTs
c Fe_2O_3/CNTs
d TiO_2/Fe_2O_3/CNTs
e TiO_2/Fe_2O_3/CNTs after one cycle
f TiO_2/Fe_2O_3/CNTs after two cycles

(UV) light and transmits visible light. From Figs. 5*b* and *c*, there is not much difference between CNTs and Fe_2O_3/CNTs in the absorption spectra. The absorption spectrum of the TiO_2/Fe_2O_3/CNTs presented in Fig. 5*d* shows a similar curve in UV light, but the adsorption is stronger than TiO_2. The absorption cutoff wavelength appears as obvious red-shift to approximately 700 nm, capable of utilising most of the visible light for photocatalysis. The reason underlying this phenomenon is that there is a straining effect existing caused by the lattice parameters difference between TiO_2 and Fe_2O_3/CNTs, the straining forced the bandgap energy of TiO_2 to the red region of the spectra [24, 25].

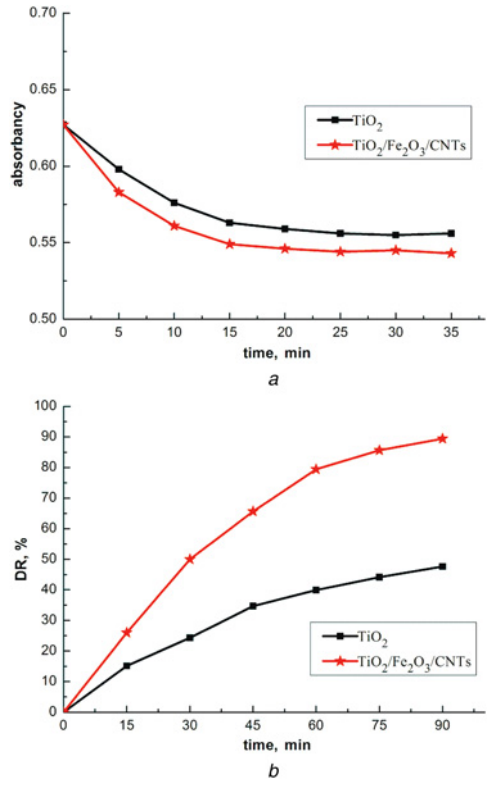

Figure 6 *Adsorption–desorption and photocatalytic degradation on tetracycline hydrochloride of two samples: TiO_2 and TiO_2/Fe_2O_3/CNTs*
a Adsorption–desorption
b Photocatalytic degradation

From the above discussion, the TiO_2/Fe_2O_3/CNTs show absorption in the visible region and are effectively excited by visible light. We demonstrated the potential application of TiO_2/Fe_2O_3/CNTs in the photocatalytic degradation of TC and the influences on photocatalysis. The degradation rate in Fig. 6 includes the adsorption of TC in the dark and photocatalytic degradation after the equilibrium. Fig. 6*a* shows that the adsorption–desorption in the dark can achieve equilibrium after 30 min. Fig. 6*b* displays the time-dependent degradation on the TC as the pollution source by TiO_2 and the TiO_2/Fe_2O_3/CNTs under the same photocatalytic degradation condition. The TiO_2/Fe_2O_3/CNTs and TiO_2 photocatalytic degradation rates are 89.41 and 47.64% in 90 min, respectively. It was well known that reducing the electron–hole recombination probability and increasing electron mobility are the key factors, the CNTs can act as an acceptor of photogenerated electrons to speed the electrons transferred from the surface of TiO_2 under visible light illumination. As a result, the electron–hole recombination was retarded and the degradability efficiency was improved.

To investigate the light catalyst reusability of the TiO_2/Fe_2O_3/CNTs, an experiment was conducted to measure the photocatalyst reuse and recycle. The process was repeated two times and the results are shown in Figs. 5*e* and *f*. It was observed that at the first time step, the degradation efficiency for the TC reached 89.41% in 90 min. After the photocatalysis, by using the methanol/acetic acid (95:5, v/v) solution eluent under an ultrasonic bath for 15 min, the degradation efficiencies for the TC reached 70.58 and 62.07% at the first and second time. Compared with the first photocatalysis, the photocatalytic capacities were reduced to 18.83 and 27.34%, respectively. It can also be seen that the total photocatalytic capacities of the TC slightly decreased with the increase of using times. From the UV–vis study in Figs. 5*e* and *f*, the ability of the absorption spectrum for the TiO_2/Fe_2O_3/CNTs decreased with the increase of using times because of the light corrosion.

4. Conclusion: In this Letter, a fast and convenient method for the preparation of TiO_2/Fe_2O_3/CNTs has been proposed. In addition, we have studied the morphology, magnetic and photocatalytic degradation of the as-prepared TiO_2/Fe_2O_3/CNTs through the different characterisation testing technologies. The results show that ferrite nanoparticles have been loaded onto the surface of the CNTs, and the TiO_2 particles were coated on the surface of the Fe_2O_3/CNTs, the photocatalysis of the composites is better than that of TiO_2 for the structure and properties of inorganic support. Moreover, we have found that TiO_2/Fe_2O_3/CNTs have better reusable photocatalysis than other traditional photocatalysts by the magnetic separation recycling method.

5. Acknowledgments: This work was supported financially by the Ph.D. Programs Foundation of the Ministry of Education of China (no. 20110205110014), the Fundamental Research Funds for the Central Universities (CHD2011TD021) and the National Training Programs of Innovation and Entrepreneurship for Undergraduates (no. 201310710055).

6 References

[1] Nie X., Wang X., Chen J., Zitko V., An T.: 'Response of the freshwater alga *Chlorella vulgaris* to trichloroisocyanuric acid and ciprofloxacin', *Environ. Toxicol. Chem.*, 2008, **27**, pp. 168–173

[2] Hoffmann M., Martin S., Choi W., Bahnemann D.: 'Environmental applications of semiconductor photocatalysis', *Chem. Rev.*, 1995, **95**, pp. 69–96

[3] Liu Y., Gan X., Zhou B., *ET AL.*: 'Photoelectrocatalytic degradation of tetracycline by highly effective TiO_2 nanopore arrays electrode', *J. Hazardous Mater.*, 2009, **171**, pp. 678–683

[4] Palominos R., Mondaca M., Giraldo A., Penuela G., Perez M.M., Mansilla H.: 'Photocatalytic oxidation of the antibiotic tetracycline on TiO_2 and ZnO suspensions', *Catal. Today*, 2009, **144**, pp. 100–105

[5] Reyes C., Fernandez J., Freer J., *ET AL.*: 'Degradation and inactivation of tetracycline by TiO_2 photocatalysis', *J. Photochem. Photobiol. A, Chem.*, 2006, **184**, pp. 141–146

[6] Hone J., Whitney M., Piskoti C., Zettl A.: 'Thermal conductivity of single-walled nanotubes', *Phys. Rev. B*, 1999, **59**, pp. 2514–2516

[7] Unger E., Graham A., Kreupl F., Liebau M., Hoenlein W.: 'Electrochemical functionalization of multi-walled carbon nanotubes for solvation and purification', *Curr. Appl. Phy.*, 2002, **2**, pp. 107–111

[8] Sun X., Zhao W.: 'Prediction of stiffness and strength of single-walled carbon nanotubes by molecular mechanics based finite element approach', *Mater. Sci. Eng. A*, 2005, **390**, pp. 366–371

[9] Qin C., Shen J., Hu Y., Ye M.: 'Facile attachment of magnetic nanoparticles to carbon nanotubes via robust linkages and its fabrication of magnetic nanocomposites', *Compos. Sci. Technol.*, 2009, **69**, pp. 427–431

[10] Azamian B., Davis J., Coleman K., Bagshaw C., Green M.: 'Bioelectrochemical single-walled carbon nanotubes', *J. Am. Chem. Soc.*, 2002, **124**, pp. 12664–12665

[11] Banerjee S., Wong S.: 'Functionalization of carbon nanotubes with a metal-containing molecular complex', *Nano Lett.*, 2002, **2**, pp. 49–53

[12] Richard C., Balavoine F., Schultz P., Ebbesen T.W., Mioskowski C.: 'Supramolecular self-assembly of lipid derivatives on carbon nanotubes', *Science*, 2003, **300**, pp. 775–778

[13] Kong H., Gao C., Yan D.: 'Controlled functionalization of multiwalled carbon nanotubes by in situ atom transfer radical polymerization', *J. Am. Chem. Soc.*, 2004, **126**, pp. 412–413

[14] An G., Na N., Zhang X., *ET AL.*: 'SnO_2/carbon nanotube nanocomposites synthesized in supercritical fluids: highly efficient materials for use as a chemical sensor and as the anode of a lithium-ion battery', *Nanotechnology*, 2007, **18**, pp. 435707–435712

[15] Baskaran D., Mays J., Bratcher M.: 'Polymer-grafted multiwalled carbon nanotubes through surface-initiated polymerization', *Angew. Chem. Int. Ed.*, 2004, **43**, pp. 2138–2142

[16] Zhao B., Hu H., Haddon R.: 'Synthesis and properties of a water-soluble single-salled carbon nanotube-poly (*m*-aminobenzene sulfonic acid) graft copolymer', *Adv. Funct. Mater.*, 2004, **14**, pp. 71–76

[17] Xie X., Gao L.: 'Characterization of a manganese dioxide/carbon nanotube composite fabricated using an in situ coating method', *Carbon*, 2007, **45**, pp. 2365–2373

[18] Lamastra F., Nanni F., Camilli L., Matassa R., Carbone M., Gusmano G.: 'Morphology and structure of electrospun $CoFe_2O_4$/multi-wall carbon nanotubes composite nanofibers', *Chem. Eng. J.*, 2010, **162**, pp. 430–435

[19] Cheng J., Zhang X., Ye Y.: 'Synthesis of nickel nanoparticles and carbon encapsulated nickel nanoparticles supported on carbon nanotubes', *J. Solid State Chem.*, 2006, **179**, pp. 91–95

[20] Chen C., Liu T., Chen X., *ET AL.*: 'Preparation and magnetic property of multi-walled carbon nanotube/α-Fe_2O_3 composites', *Trans. Nonferrous Mel. Snc.*, 2009, **19**, pp. 1567–1571

[21] Korneva G., Ye H.H., Gogotsi Y., *ET AL.*: 'Carbon nanotubes loaded with magnetic particles', *Nano Lett.*, 2005, **5**, pp. 5879–884

[22] Komogortsev S., Iskhakov R., Denisova E., Balaev A., Myagkov V., Bulina N.: 'Magnetic anisotropy in the films of oriented carbon nanotubes filled with iron nanoparticles', *Tech. Phys. Lett.*, 2005, **31**, pp. 454–456

[23] Neppolian B., Choi H., Sakthivel S., Arabindoo B., Murugesan V.: 'Solar/UV-induced photocatalytic degradation of three commercial textile dyes', *J. Hazard. Mater.*, 2002, **89**, pp. 303–317

[24] Smith A., Mohs A., Nie S.: 'Tuning the optical and electronic properties of colloidal nanocrystals by lattice strain', *Nat. Nanotechnol.*, 2009, **4**, pp. 56–63

[25] Maki H., Sato T., Ishibashi K.: 'Direct observation of the deformation and the band gap change from an individual single-walled carbon nanotube under uniaxial strain', *Nano Lett.*, 2007, **7**, pp. 890–895

doi: 10.1049/mnl.2013.0428